

Channel Models for Capacity Evaluation of MIMO Handsets in Data Mode

Nielsen, Jesper Ødum; Yanakiev, Boyan; Barrio, Samantha Caporal Del; Pedersen, Gert Frølund

Published in:
I E T Microwaves Antennas & Propagation

DOI (link to publication from Publisher):
[10.1049/iet-map.2015.0769](https://doi.org/10.1049/iet-map.2015.0769)

Creative Commons License
Other

Publication date:
2017

Document Version
Early version, also known as pre-print

[Link to publication from Aalborg University](#)

Citation for published version (APA):
Nielsen, J. Ø., Yanakiev, B., Barrio, S. C. D., & Pedersen, G. F. (2017). Channel Models for Capacity Evaluation of MIMO Handsets in Data Mode. *I E T Microwaves Antennas & Propagation*, 11(1), 1-9.
<https://doi.org/10.1049/iet-map.2015.0769>

General rights

Copyright and moral rights for the publications made accessible in the public portal are retained by the authors and/or other copyright owners and it is a condition of accessing publications that users recognise and abide by the legal requirements associated with these rights.

- Users may download and print one copy of any publication from the public portal for the purpose of private study or research.
- You may not further distribute the material or use it for any profit-making activity or commercial gain
- You may freely distribute the URL identifying the publication in the public portal -

Take down policy

If you believe that this document breaches copyright please contact us at vbn@aub.aau.dk providing details, and we will remove access to the work immediately and investigate your claim.

Channel Models for Capacity Evaluation of MIMO Handsets in Data Mode

Jesper Ødum Nielsen¹, Boyan Yanakiev², Samantha Caporal Del Barrio¹, Gert Frølund Pedersen¹

¹APNet, Dept. of Electronic Systems, Faculty of Engineering and Science, Aalborg University, Niels Jernes Vej 12, DK-9220 Aalborg, Denmark. Email: {jni, scdb, gfp}@es.aau.dk

²Intel Mobile Communications Denmark Aps (Aalborg), Alfred Nobels Vej 25 DK-9220 Aalborg, Denmark. Email: boyan.yanakiev@intel.com

Abstract: This work investigates different correlation based models useful for evaluation of outage capacity (OC) of mobile multiple-input multiple-output (MIMO) handsets. The work is based on a large measurement campaign in a micro-cellular setup involving two dual-band base stations, 10 different handsets in an indoor environment for different use cases and test users. Several models are evaluated statistically, comparing the OC values estimated from the model and measurement data, respectively, for about 2,700 measurement routes. The models are based on either estimates of the full correlation matrices or simplifications. Among other results, it is shown that the OC can be predicted accurately (median error typically within 2.6%) with a model assuming knowledge only of the Tx-correlation coefficient and the mean power gain.

1. Introduction

In currently evolving long-term evolution (LTE) and LTE Advanced cellular systems, MIMO technology is used to provide improved link throughput and network capacity, compared to previous generations of cellular systems [1]. It is well known that the MIMO technology in general is depending on the mobile radio channel in providing multiplexing gain and diversity, see *e.g.*, [2]. For the important case of handheld devices in cellular systems, it has been known for more than a decade that the radio channel is highly influenced by the user, as demonstrated via measurements for the single-input single-output (SISO) case in, *e.g.*, [3, 4] and later for the MIMO case in [5–7].

Unsurprisingly, the design of the handset, *i.e.*, the antennas and their location on the handset, as well as other parts of the handset, may have a significant influence on the capacity or throughput [8–11]. Hence, optimisation of handset designs is an important issue in ensuring the best performance of handsets in terms throughput and coverage.

One straightforward way to evaluate an actual product or prototype is to use field measurements, as in, *e.g.*, [10] where the capacities of some handsets are derived from measurements in a base station (BS) to indoor scenario. However, in many cases such a procedure is both difficult to reproduce and costly, and hence undesirable as part of a design procedure where many iterations on the design may be needed. Other examples of field measurements include [12, 13], testing some automotive antennas in LTE networks.

In order to avoid the cumbersome direct field measurements, it is necessary to find some way to separate the radio propagation in the mobile environment from the antenna system. Hence a model of the channel is needed, such as the one proposed in [14] based on abstract model assumptions. The model may incorporate correlation at both the transmitter and receiver ends and is useful for providing insight into key propagation parameters governing the performance. Also using abstract models of the environment, the work in the references [15–18] derive under varying assumptions the spatial correlation properties for a given base station antenna setup in a idealized, site-unspecific geometrical setup. The spatial correlation is known to be an important parameter in the MIMO system performance and hence the results provide valuable insights. However, when trying to evaluate the performance of a given handset design, results of these works are not immediately applicable, since the handset antenna properties may be unknown or very difficult to establish when a user is involved with a possibly dynamic impact.

For simulation of channels, one approach is to use a geometric-stochastic model, such as the so-called spatial channel model extended (SCME), or the model from the WINNER project [19, 20], where a hypothetical random channel is imposed on the antenna system. As an alternative to simulation, the channel can also be obtained with ray-tracing where the propagation paths are obtained from computations using physical models of the environment, see for example [21]. In principle a powerful approach, but limited by computational complexity and availability of accurate physical models.

In over the air (OTA) testing, a final product, prototype or mockup device is evaluated by exposing the antenna system to an emulated channel. A full transceiver system is employed, using *e.g.* an LTE BS, and in principle any channel model can be emulated, given a sufficient number of probes and channel emulator channels [22–24]. Since OTA testing involves not only the antennas but also full transceivers, it is the complete system that is tested, including any adaptive arrays such as discussed in [25]. It is possible to include user aspects, *e.g.*, by including a user phantom or live user during the channel emulation. However, emulating the channel accurately when both the antenna system and the user is present may require a large and expensive hardware setup [26].

As an alternative to the generic SCME type of models, site-specific channel models have been used for antenna system performance, as demonstrated in [6, 27]. Using measurements performed with antenna arrays, plane waves are estimated as they change, *e.g.*, along a route. Assuming the radiation patterns of the antennas are known, this method also allows experimentation with different antenna designs and figure of merits in a reproducible way. Alternatively, the site specific models can in principle be used in an OTA setup, as mentioned above. It is possible to include user aspects, but this likely requires that the user is considered together with the antenna system, for example by measuring or simulating the radiation patterns of the antennas while the user is holding the device. Such measurements have been demonstrated, at least for SISO systems, in [28–30]. However, in this way any dynamic user aspects are not easily included. Further, in this type of models the antennas are assumed to be in the far field of the propagation environment.

Although the performance of a MIMO handset in general depends on all properties of the channel matrix, the results presented in [31] showed that for realistic handsets and use, the received power is by far the most significant figure of merit to optimise, as compared to correlation and branch power ratio (BPR). With this in mind, the objective of the current work has been to investigate to what degree details of the channel properties are necessary to predict the channel capacity for realistic designs and use of handsets. To this end, the large set of measurements described in [31] has been analyzed and different types of MIMO channel models have been investigated, all zero-mean Gaussian but with different assumptions on the correlation properties. While these are

well known model types, the novelty of the current work lies in their evaluation using highly realistic propagation data, allowing a joint inclusion of model structure, handset properties, environment and user influence.

As shown in the following sections, the statistics of the channel capacity obtained with different handsets can be approximated well using knowledge only about the mean received power and correlation between Tx-branches. Hence, an approximate capacity evaluation of a given design may potentially be carried out in much simpler ways than with the methods described above.

Although the current work focuses mainly on the accuracy in the modeling rather than the performance of the individual handsets, it should be noted that the modeling results are obtained with a set of handsets performing widely different in terms of capacity. More detailed results on the handset performances are presented in [31,32].

It is important to note that the capacity is a theoretical upper limit that may not be achieved in a given system architecture. Therefore, the performance evaluation proposed in the current work is not a replacement for carrying out performance evaluation in, *e.g.*, an OTA setup targeting a specific system and implementation. Instead, the idea is to provide a system independent performance evaluation which is relatively easy to obtain and use as part of a design procedure.

The rest of this paper is organised with the measurements described in Section 2 and the data processing and figures of merits defined in Section 3. The results are discussed in Section 5, followed by conclusions in Section 6.

2. Measurements

The results presented in this paper are based on a measurement campaign carried out in the City of Aalborg, Denmark. The campaign is described in detail in [31], while a brief overview is given here.

A micro-cellular setup was used with two BSs, BS1 and BS2 (see Fig. 1) and with the mobile stations (MSs) on the top floor of a three-story office building. Both BSs were equipped with four antennas, two for each of the bands 796 MHz and 2300 MHz, denoted the low band (LB) and high band (HB), respectively. BS1 had obstructed line of sight (LOS) to the measurement building, located about 150 m away, and was about the same height as the nearest buildings. BS2 was overlooking the surroundings, located on top of a tall building at a height of about 60 m.

The MS location was inside a large hallway/common room on the 3rd floor of a building mainly made of concrete. All measurements were made inside or around four squares with 1 m side length, as illustrated in Fig. 2. During the measurements the user moved randomly inside the square, but kept the same posture and orientation. Four users were measured at the same time, each in a separate square and where the relative orientation of the users were 0° , 90° , 180° and 270° , respectively.

In total ten mock-up handsets have been used, each designed to be realistic with respect to antenna shape and size, as well as casing and handling. An accurate manufacturing of all the handsets in PC-ABS plastics was obtained by utilizing a 3D rapid prototyping printer. Using an optical fibre connection [33], the handsets were connected to the sounding equipment without altering the electromagnetic properties of the devices. The handsets are widely different, with some designed to mimic typical devices on the market and some more experimental.

In the following the handsets are labelled H1, H2, ..., H6, H11, H12, H13. Note that H14 was omitted from the work related to the current paper due to rights issues. All handsets have two dual band antennas, except H3 and H4 having only a single antenna on the LB, and H13 which is LB

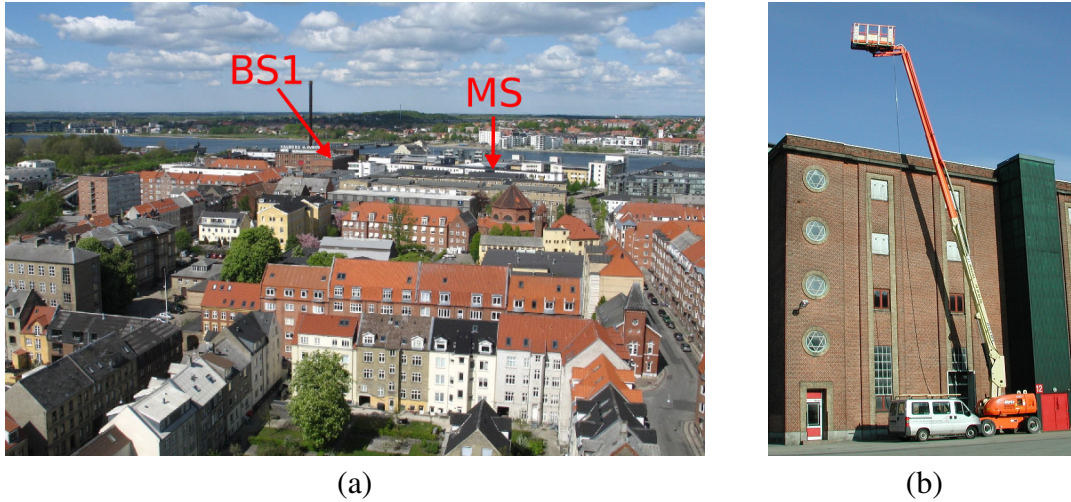


Fig. 1. (a) View from BS2 towards the measurement location. (b) BS1 mounted on lift [31].

only.

The different handsets were measured in groups of four in free space (FS), with phantoms, and with users. Different use cases (UCs) were measured, all in *data mode*, *i.e.*, when the user holds the handset in front of the body, as if reading or browsing. The included UCs are: landscape mode for left (LRHL), right (LRHR), and two hands (LRTH), and in portrait mode with right hand (PHR) and two hands (PTH). In addition, corresponding FS measurements were made with the handsets mounted on expanded polystyrene (EPS) at an angle of 45° . All handsets were measured with 4–8 users for each UC. In addition, many measurements were repeated.

The measurements were obtained using a wideband MIMO channel sounder [34], allowing simultaneous measurements of the channels from all four LB and four HB transmitter (Tx) antennas on the two base stations, to four dual-band receiver (Rx) antennas. Using additional 1:2 switching, a 8×16 MIMO (Tx \times Rx) wide band channel matrix was measured at a rate of 60 Hz to cope with channel changes due to the movements of the users and other changes in the channel.

In total more than 1,000 measurement runs were carried out, resulting in a total of more than 12,000 valid MIMO channel measurements. Though the measurements are wideband, the work presented in this paper is based on narrow band data, obtained via discrete Fourier transforms.

3. Data Processing

Four different MIMO constellations are considered. BS1LB denotes the constellation where two LB Tx branches from BS1 are used to form a 2×2 MIMO setup for each handset. Similarly, BS1HB uses the HB from BS1, while BS2LB and BS2HB are the LB and HB channels originating from BS2, respectively.

The MIMO channel is described by the matrix $H_i^r(m)$ consisting of the elements $h_i^r(p, q, m)$ where indices denote, respectively, the p -th Rx antenna branch, the q -th Tx antenna branch, and the m -th time index. The i -index specifies a combination of the MIMO constellation, handset, orientation/location, repetition number, user, and UC, where each combination results in a different MIMO channel measurement. For brevity, the combination details are omitted in the following description. The superscript r indicates a un-normalised measurement. The scalar $h_i^r(p, q, m)$ is the complex gain of the narrow-band channel between the Tx and Rx branches.

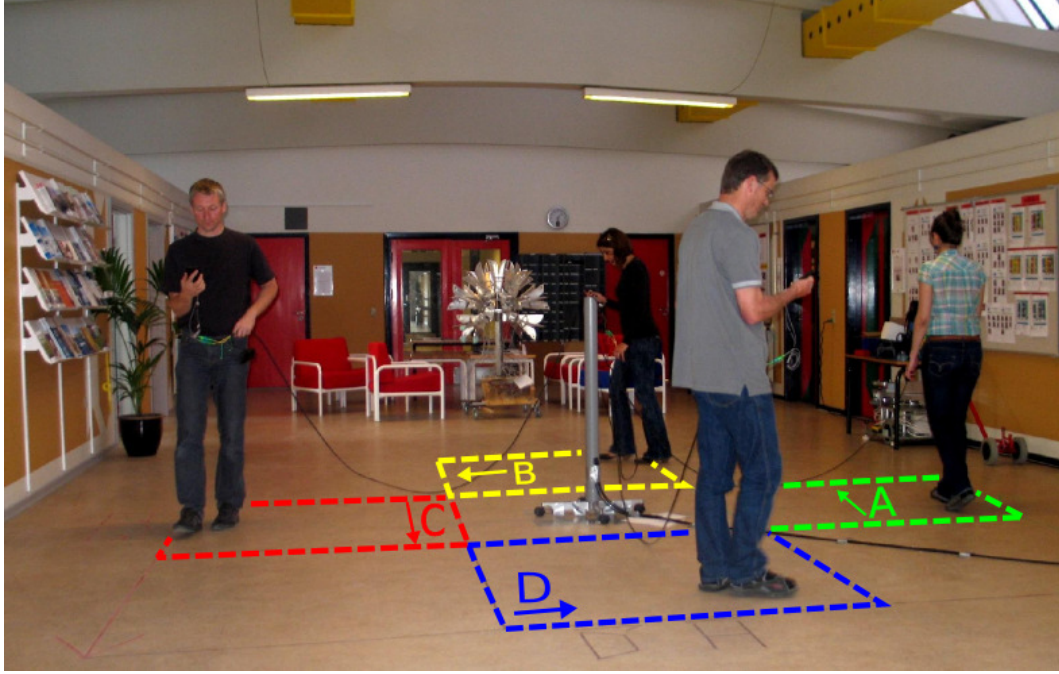


Fig. 2. Users during measurements, with the user squares and orientations A–D indicated [31].

To ensure a fair comparison, the channels are normalised to the mean power of all handsets in FS. The FS average power gain for the q -th Tx branch is computed as

$$\Lambda(q) = \frac{1}{PMI} \sum_{p=1}^P \sum_{m=1}^M \sum_{i=1}^I |h_i^r(p, q, m)|^2 \quad (1)$$

where $P = 2$ is the number of Rx branches of the handsets, and $M = 1200$ is the number of narrow-band samples in each measurement. The averaging is done over I combinations of handset, orientation, UC, *etc.* The normalised channel matrix $H_i(m)$ has the elements

$$h_i(p, q, m) = \frac{h_i^r(p, q, m)}{\sqrt{\Lambda(q)}} \quad (2)$$

for the m -th time index and a handset in the i -th combination. $H_i(m)$ is the $P \times Q$ random channel matrix, where P and Q are the numbers of Rx and Tx antennas, respectively. Assuming that the transmitter has no knowledge of the channel and no interference is present, the capacity of the channel is given by [2]

$$c_i(m) = \sum_{e=1}^E \log_2 \left(1 + \frac{\lambda_i(e, m) \rho}{Q} \right) \quad (3)$$

where $\lambda_i(e, m)$ is the e -th eigenvalue of the matrix $H_i(m)H_i(m)^H$ and ρ is the signal to noise ratio (SNR). Note that ρ is defined relative to the normalisation in (2).

The channel is considered statistically stationary during each measurement in the following, since the user moves only within a small area and keeps the same orientation and posture. Thus, the $M = 1200$ samples obtained in each measurement are random samples of the channel due to

small-scale changes. The OC χ_i^α is used to characterise the channel, where α is the probability level and the i -index denotes the combination of handset, user, UC, and orientation.

The aim of this work is to find channel models useful for predicting the OC. To this end the following error measure is used,

$$\varepsilon_i^\alpha = \frac{\chi_i^\alpha - \tilde{\chi}_i^\alpha}{\chi_i^\alpha} \quad (4)$$

where $\tilde{\chi}_i^\alpha$ is the OC obtained with the model. The terms in (4) are regarded as random, since the OCs depend on the random channel, as well as the specific combination indicated by the i -index. The errors in the predicted OCs are therefore analyzed using percentiles of $|\varepsilon_i^\alpha|$ or using boxplots of ε_i^α .

4. Channel Models

All the channel models considered are based on the relation

$$\text{vec}[H(m)] = R_H^{1/2} \text{vec}[G(m)] \quad (5)$$

where $G(m) \in \mathcal{C}^{P \times Q}$ is a matrix of independent, zero-mean Gaussian random variables of variance one, and $\text{vec}(\cdot)$ denotes stacking of the columns of the matrix argument. The matrix $R_H \in \mathcal{C}^{PQ \times PQ}$ defines the average power and the correlation coefficients (CCs) between all channel coefficients in H . It is assumed in the following that the power is normalised, so that the diagonal elements of R_H are all one.

For a 2×2 MIMO channel, the R_H matrix can be written as

$$\begin{bmatrix} c_{11,11} & c_{11,21} & c_{11,12} & c_{11,22} \\ c_{21,11} & c_{21,21} & c_{21,12} & c_{21,22} \\ c_{12,11} & c_{12,21} & c_{12,12} & c_{12,22} \\ c_{22,11} & c_{22,21} & c_{22,12} & c_{22,22} \end{bmatrix} = \begin{bmatrix} 1 & r_1 & t_1 & s_1 \\ r_1^* & 1 & s_2 & t_2 \\ t_1^* & s_2^* & 1 & r_2 \\ s_1^* & t_2^* & r_2^* & 1 \end{bmatrix} \quad (6)$$

where $c_{pq,p'q'} = \mathcal{E}\{h(p,q,m)h^H(p',q',m)\}$ is the desired CC between the channels with index pairs (p,q) and (p',q') , and where $\mathcal{E}\{\cdot\}$ is the expectation operator. Given the zero-mean Gaussian channel assumption, the model is completely determined by the six complex parameters in (6), where t_1 and t_2 are the Tx-correlation coefficients (TxCCs), r_1 and r_2 are the Rx-correlation coefficients (RxCCs), and s_1 and s_2 are the cross-link correlation coefficients (LxCCs).

The current work investigates different models based on (5), assuming the branch mean power is known, so that only the correlation matrix (6) needs to be defined. The mean branch power is estimated from the measured data as

$$\gamma(p,q) = \frac{1}{M} \sum_{m=1}^M |h_i(p,q,m)|^2 \quad (7)$$

i.e., the average power during the measurement. The CC matrix (6) is then estimated as

$$\tilde{c}_{pq,p'q'} = \frac{\sum_{m=1}^M h_i(p,q,m)h_i^*(p',q',m)}{M\sqrt{\gamma(p,q)\gamma(p',q')}} \quad (8)$$

omitting the combination index i . In (8) and below the tilde ('~') is used to designate an estimated value, *e.g.*, when referring to the estimated TxCC for the first Tx branch as \tilde{t}_1 .

The overall objective of this work is to identify models that are useful for evaluating the OCs of handsets sufficiently accurate, while being practical in the sense of only requiring parameters that may be obtained without propagation measurements with the handset being evaluated. To this end, several different variations of the CC matrix are assumed in the model from (5). For each channel configuration, the complete CC matrix is estimated, from which the most accurate model (*FullCovMat*, see below) may be formed. This model is not very useful for evaluation of handset OCs, since the model parameters are typically only available via propagation measurements with the handset, in which case the modeling is superfluous. However, the model may serve as a reference case. By simplifying the *FullCovMat* model, several different, less accurate models are obtained, as described below. These models allow investigation of the tradeoff between OC estimation accuracy and model complexity.

FullCovMat This is the most generic and complex case where all the values $t_1, t_2, r_1, r_2, s_1, s_2$ may be different and are estimated using data from the individual channels.

Kronecker A special case where the CC of the Rx channels is assumed independent of the Tx, and vice versa. The CCs are estimated as $r = r_1 = r_2 = (\tilde{r}_1 + \tilde{r}_2)/2$, and $t = t_1 = t_2 = (\tilde{t}_1 + \tilde{t}_2)/2$. Further, $s_1 = tr$ and $s_2 = r^*t$, see [35].

NoRxCorr The Rx channels are uncorrelated, $r_1 = r_2 = 0$; the other coefficients t_1, t_2, s_1 , and s_2 are estimated from the measured data.

NoLxRxCorr The Rx channels are uncorrelated, $r_1 = r_2 = 0$, and also the LxCCs are assumed to be zero, $s_1 = s_2 = 0$. The TxCC coefficients, t_1 and t_2 , are estimated from the measured data.

FixTx0.25 A fixed value is assumed for the TxCC; $t_1 = t_2 = 0.25$. The RxCCs and LxCCs are assumed zero; $r_1 = r_2 = s_1 = s_2 = 0$.

FixTx0.8 A fixed value is assumed for the TxCC; $t_1 = t_2 = 0.8$. The RxCCs and LxCCs are assumed zero; $r_1 = r_2 = s_1 = s_2 = 0$.

NoTxRxCorr Both the Tx and Rx channels are uncorrelated, $t_1 = t_2 = r_1 = r_2 = 0$; the coefficients s_1 and s_2 are estimated from the measured data.

NoCorr All channels are uncorrelated; $t_1 = t_2 = r_1 = r_2 = s_1 = s_2 = 0$.

Detailed statistics on the TxCC, LxCC, and RxCC were presented in [32], based on the same measured data set as used in the current work. Fig. 3 shows the median values of the three types of CCs for all combinations of handsets and MIMO constellations. Although the shown correlation statistics may give a hint of which of the above listed models can be expected to be accurate, the models must be evaluated by comparing the obtained capacity values, modeled and measured. In this way any differences are included, *e.g.*, those due to an incorrect model structure or due to the near-field influence by the individual user causing dynamic changes in, *e.g.*, the BPR and the correlation levels.

For each combination of MIMO constellation, UC, user, and orientation one or more measurement runs are available. Based on each run of $M = 1200$ samples, the OC was estimated. In addition, the average powers of the channel matrix were estimated, using (7), and the CCs using (8). Each of the models listed above was then simulated using 10^4 realisations, from which the

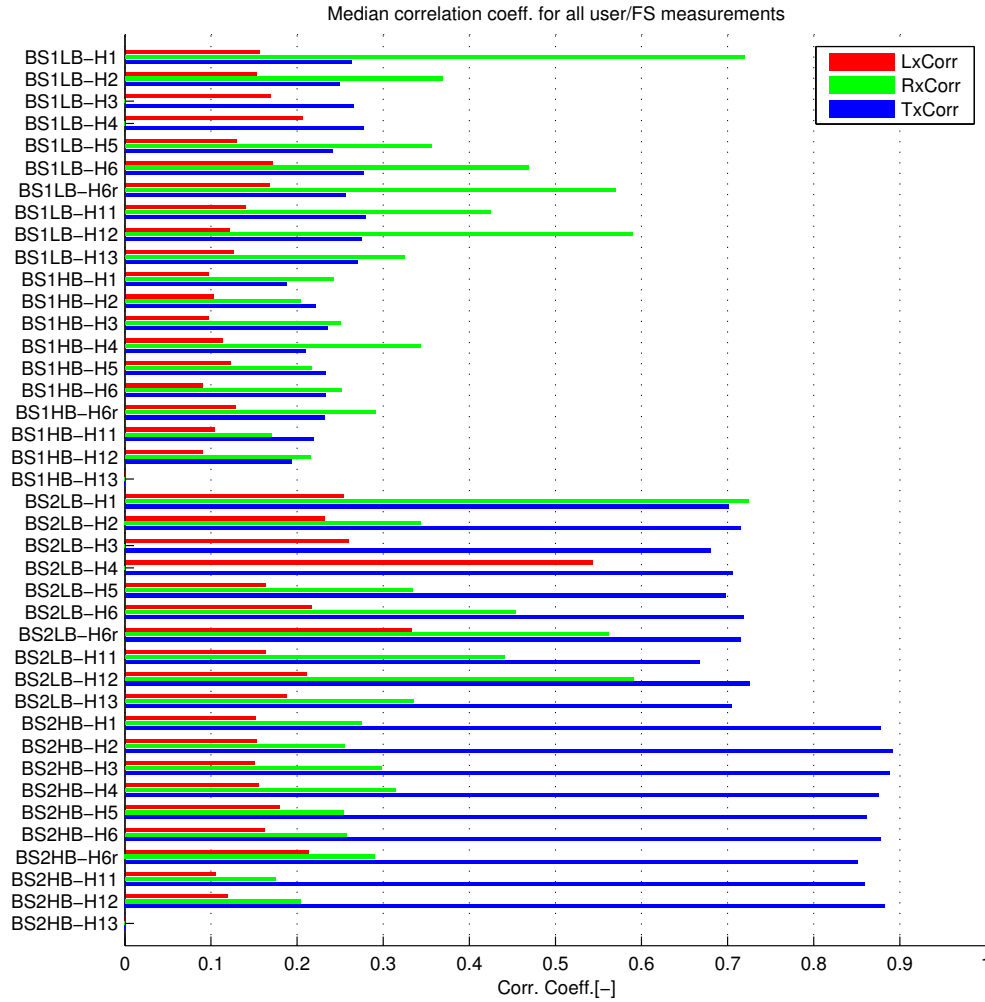


Fig. 3. Median RxCC, TxCC, and LxCC obtained from all measurements with different users and in FS for all orientations and UCs.

corresponding OC values, $\tilde{\chi}_i^\alpha$ were obtained. The previous steps were then repeated for each of the I combinations of UC, user, *etc.*, and the subsequent statistics are based on these.

About 2,700 measurements, were obtained in total, of which about 950 were measured in landscape mode with a user, about 650 were in portrait mode with a user, and about 1,100 were in FS. Each of the handsets were measured 122–589 times, depending on the handset.

With the simple method described above there is no guarantee that the constructed CC matrices are positive definite, and thus valid for simulations of the model. Measurements corresponding to negative definite matrices are simply omitted from the statistics. For the NoRxCorr model many of the constructed covariance matrices are negative definite, with the H4/BS2LB channels as extremes where only about 10% of the models are useful. This may also be seen as an indication that this model is highly artificial. For all the other models, more than 99% of the matrices were positive definite.

As an alternative to simulations of the models, one might consider obtaining the associated OCs using analytical formulas, *e.g.*, as derived in [36]. However, the simulation approach was chosen, as it seemed simpler in practice and not all types of models are covered by the work in [36].

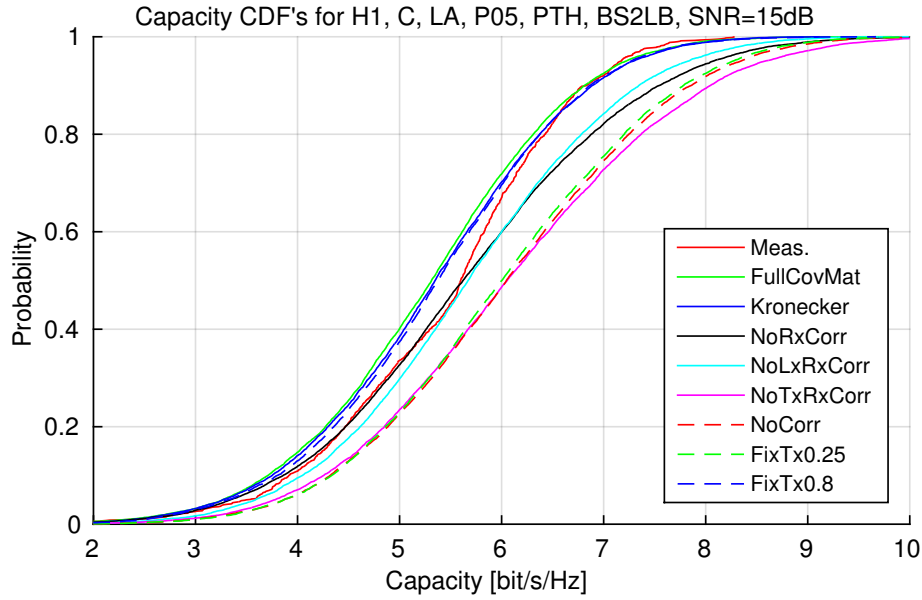


Fig. 4. cumulative distribution functions (CDFs) for both measured data and different models with estimated parameters. Note the x-axis has been limited to 2–10 bit/s/Hz.

5. Results

Examples of the obtained channel capacity CDFs are shown in Fig. 4 for a particular combination of handset UC, user, orientation, MIMO constellation and for an SNR of 15 dB. The figure shows that the FullCovMat, Kronecker, and FixTx0.8 models result in almost identical CDFs which are in general closest the CDF for the measurements, although none of the models results in a fit for all levels.

The difference between the OC obtained with a model and the OC obtained with the measured data tends to be increasing with the SNR, but at a lower rate than the OC, leading to a generally decreasing relative error. However, the model error depends on both the model type, the SNR and the outage capacity level (OCL).

The relative error ε_i^α defined in (4) is used as a measure of the model fitness to a measurement for a given combination of handset, UC, user, orientation, and MIMO constellation. With the purpose of evaluating the overall suitability of each model, ε_i^α is computed for all the available measurements and the 90%-percentile of the $|\varepsilon_i^\alpha|$ values obtained with the different measurements is used to measure the fitness of the model to the data.

Below, the dependence of the relative modeling error on the SNR is firstly studied and, secondly, the relative error versus the OCL is studied. In both cases, statistics based on all handsets are used. Following this, the performance of the NoLxRxCorr model is studied individually for each handset and MIMO constellation.

Fig. 5 shows the 90% percentile of the relative error versus SNR for a 50% OCL, for all the MIMO constellations and the different models. From the plots, some overall tendencies are commented below.

Since the FullCovMat model allows the closest fit to the individual measurements, it is not surprising that this model often results in the lowest error. In comparison, the Kronecker model

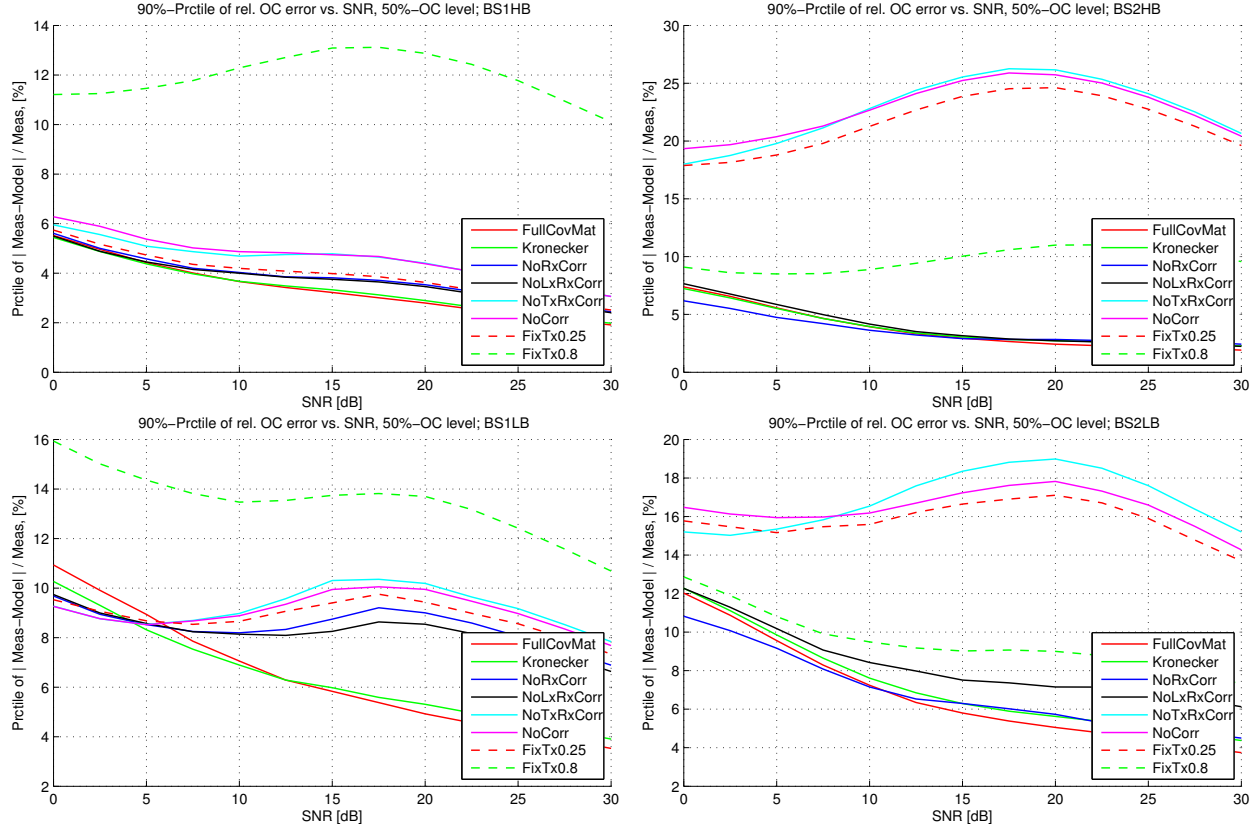


Fig. 5. 90%-percentile of model errors versus SNR for an outage capacity level (OCL) of 50%. The statistics are computed based on measurement data from all combinations of handsets, UCs, orientations, and users.

has a smaller number of parameters but the overall performance is often close to that of the FullCovMat model. Thus, the assumption of independence of the TxCC on the Rx branch and vice versa seems confirmed, if only indirectly.

The results for the different models depend highly on the MIMO constellation and hence the channel properties. For the channels involving BS1 the median TxCC is typically low, less than 0.3, as seen from Fig. 3. In these cases, using the FixTx0.8 model leads to the largest relative errors, while the FixTx0.25 model yields results similar to that of the other models, except the FullCovMat and Kronecker models for the BS1LB constellation. Apart from these two, all the models assume an RxCC of zero, which is often not correct for the LB, and therefore larger relative errors are typically found for these models in this band.

For the channels involving BS2, the median TxCC is with few exceptions higher than 0.7, which explains that the models with assumed zero or low TxCC leads to the largest relative errors. For the BS2HB constellation, it seems that using the correct TxCC of the model is the most important issue, as the FullCovMat, Kronecker, NoRxCorr, and NoLxRxCorr models all give similar results for this constellation. This may be explained by the generally low RxCC and LxCC, where median values are lower than about 0.3 in all cases (see Fig. 3). A larger discrimination among the models is noticed for the BS2LB constellations, where especially the median RxCC is somewhat higher than for the BS2HB constellations.

Fig. 6 shows the relative error in the OC versus the OCLs and a fixed SNR of 15 dB. A general

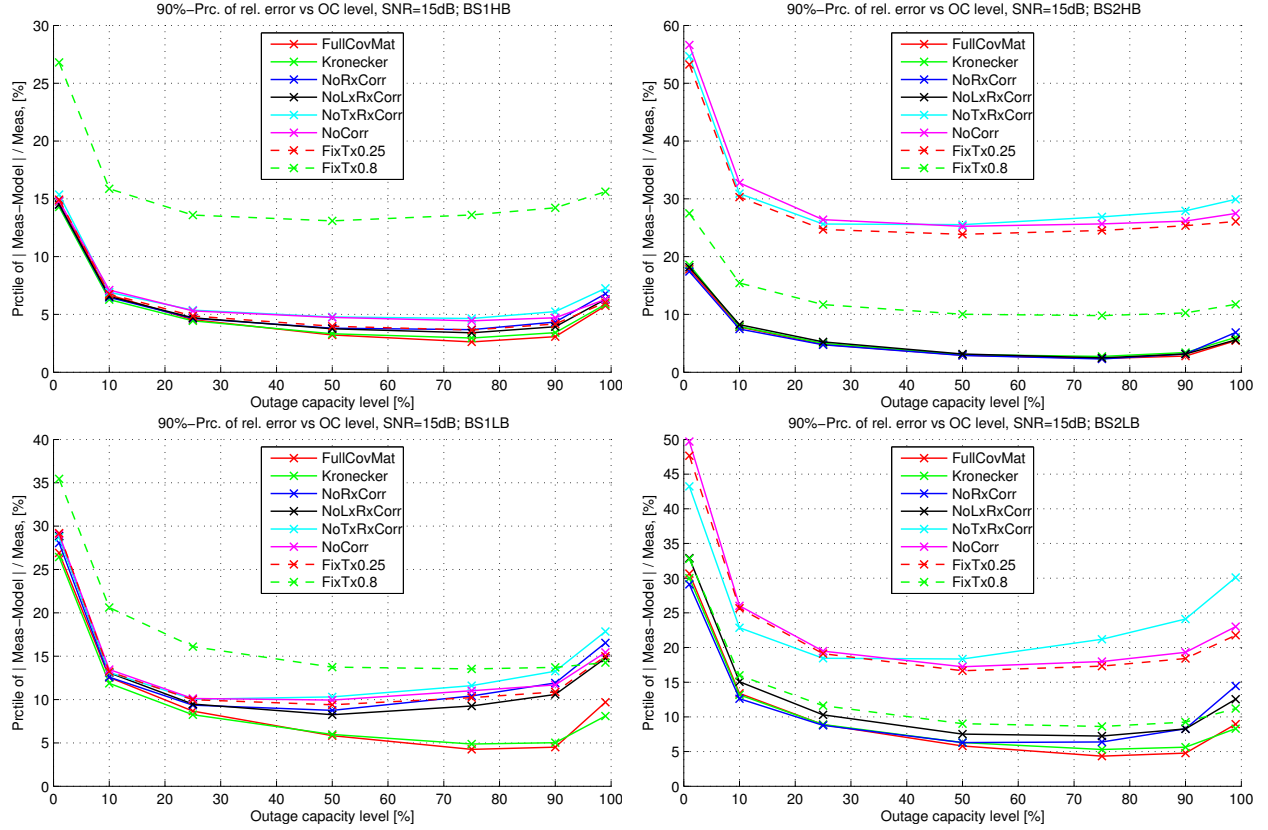


Fig. 6. 90%-percentile of model errors versus OCL, for an SNR of 15 dB. The statistics are computed based on measurement data from all combinations of handsets, UCs, orientations, and users.

tendency is that the relative error increases towards the ends of the curves, *i.e.*, increasing or decreasing OCL. In other words and as might be expected, the capacity distributions resulting from the channel models are best in an interval around the median OC.

A major contribution of this work is that, concluding on the results mentioned above, it seems that in many cases both the RxCC and the LxCC are small and not very important from a modeling point of view, whereas using the correct TxCC is more critical for obtaining a low error in the modeled OC. Based on these observations, the NoLxRxCorr is studied further in order to see the variation among the handsets in the modeling error.

In the plot of Fig. 7, each box with associated horizontal lines represent a handset and MIMO constellation combination where the median OC is shown as the middle line inside the box, and the 25%-percentile Q_1 and 75%-percentile Q_3 as left and right vertical lines of the box, respectively. Data shown as ‘+’ are outliers, defined as data points deviating more than $1.5 \times (Q_3 - Q_1)$ from the nearest percentile, Q_1 or Q_3 . The dashed lines indicate the extend of the data which are not outliers. Note that the relative error $\varepsilon_i^{50\%}$ is signed.

The majority of the modeled $\varepsilon_i^{50\%}$ values are within $\pm 10\%$, with the most significant exceptions occurring with H1 on the LB, with median errors up to -6.7% . For the remaining handsets the median errors are within $\pm 2.6\%$ for the LB. The modeling errors are generally smaller for the HB, where the median values are within $\pm 1.9\%$ for all the handsets.

The large errors obtained with H1 are explained by the generally large RxCC values estimated from the measurements with this handset. With median values about 0.7 (see Fig. 3), a channel

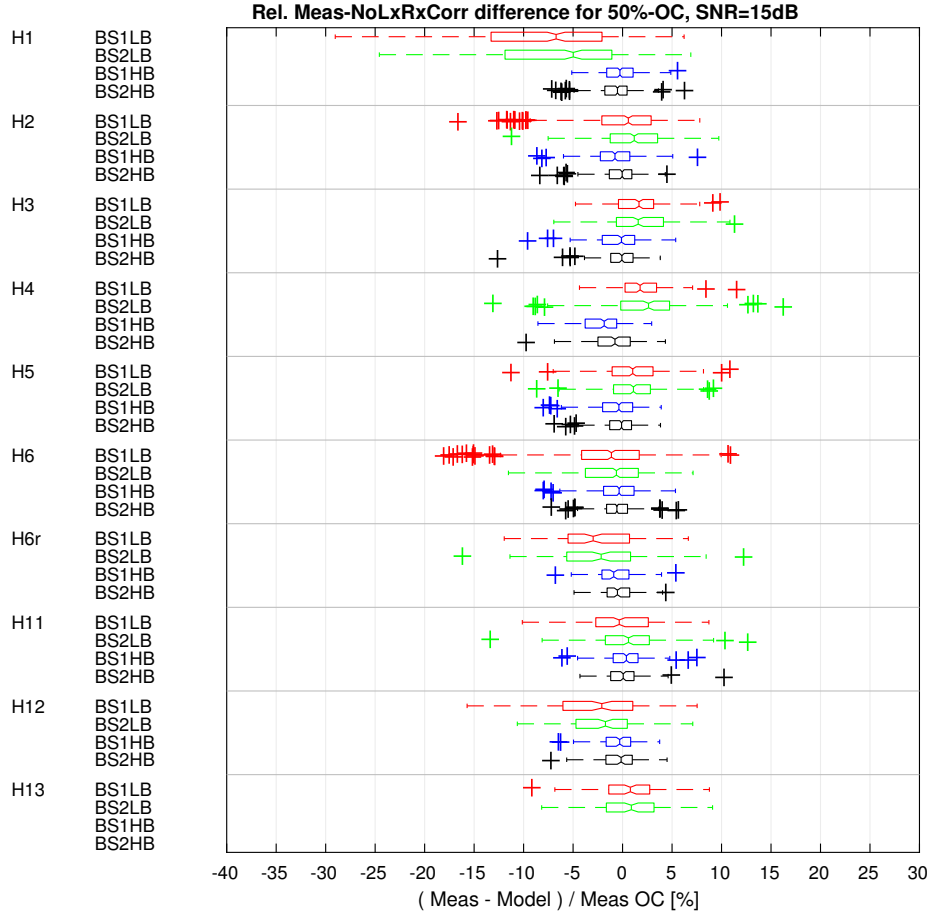


Fig. 7. Statistics (boxplot) of relative error $\varepsilon_i^{50\%}$ in modeling the median capacity using the NoLxRxCorr model and for an SNR of 15 dB. All combinations of handsets and MIMO constellations (shown with color).

model assuming zero correlation leads to a poor fit.

The above results are for an SNR of 15 dB, where Fig. 5 indicates that in general the error increases with decreasing SNR. However, it is not a dramatic increase and the plots similar to Fig. 7 for SNR 5 dB, 10 dB and 20 dB all have the majority of errors within $\pm 10\%$. Fig. 8 shows the errors for an SNR of 5 dB.

The maximum median error were up to 5.1%, -4.7% , and -7.3% for SNRs of 5 dB, 10 dB, 20 dB, respectively.

5.1. Repeatability

For practical measurements it is unavoidable that the actually acquired data differs from what would be obtained in the ideal situation, due to minor deviations from the intended scenario, measurement noise, estimation error, changes in the environment, *etc.*

In order to gain insight into the uncertainty caused by such sources, the following investigation is carried out, similar to what was done in [31] for, *e.g.*, the BPR. Here, the median OC for a 15 dB SNR is considered. A number of repeated measurements are used, namely the data mode

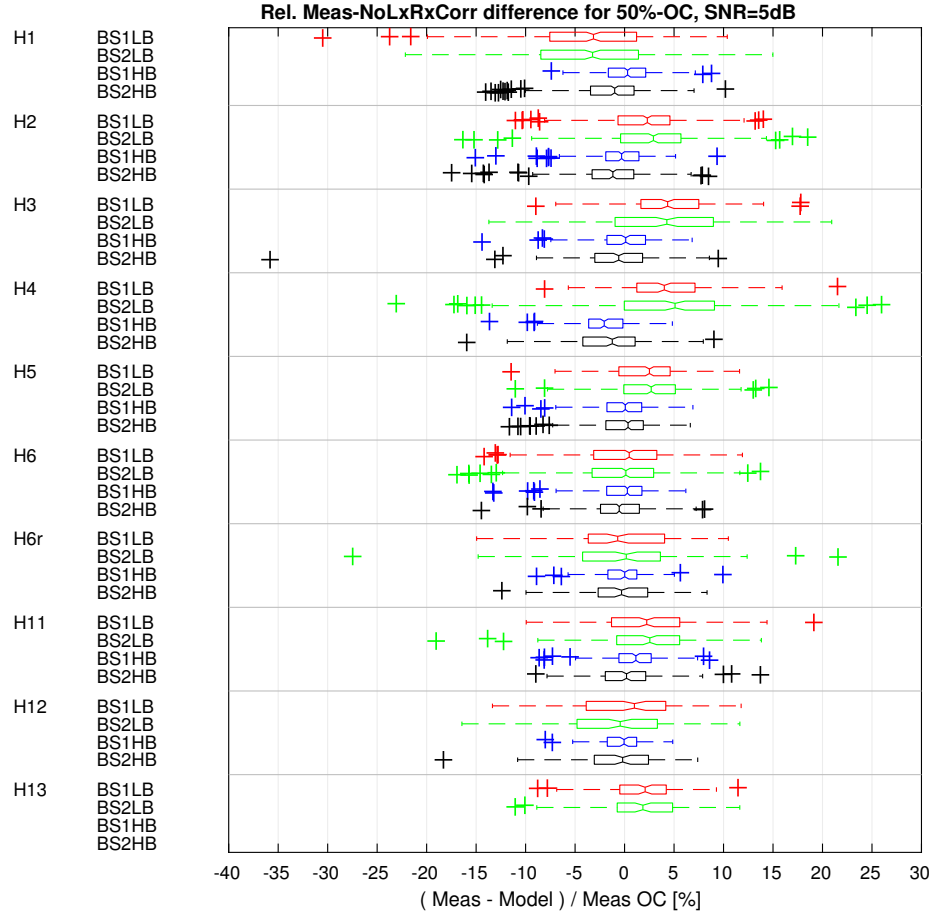


Fig. 8. Statistics (boxplot) of relative error $\varepsilon_i^{50\%}$ in modeling the median capacity using the NoLxRxCorr model and for an SNR of 5 dB. All combinations of handsets and MIMO constellations (shown with color).

portrait (DMP) UC emulated in FS by mounting the handsets on a block of expanded polystyrene (EPS) at an angle of 45° . The block of EPS with the handsets is on top of a wheeled table. During the measurements the table is moved randomly within each one of the different squares, A–D. Repeated measurements with the handsets H6, H1, H2, and H5 were obtained in this way and all combinations of the four squares and the four handsets are included.

For every combination of MIMO constellation, handset, and square, all the repeated measurements are collected and the channel model parameters are estimated, as described above. For both the measured data and the models the OCs are obtained. The repeated measurements result in random samples of these quantities which are normalised with the sample mean of the particular combination. The normalised values are grouped together and percentiles are estimated.

Table 1 shows the results for the different models and MIMO constellations, where the 50% OC for a 15 dB SNR is considered. The percentiles are based on 376 measurements, except for the NoRxCorr model where only 193 and 57 for the BS1HB and BS2HB, respectively. The smaller number of samples for this model is due to the frequent case of negative definite covariance matrices, as explained above.

In general the table shows relatively small deviations, where the HB percentile is always

Table 1 Percentiles for deviations from mean model error in 50% OC, computed from repeated measurements with different handsets and orientations.

Model	Percentile	BS1LB	BS2LB	BS1HB	BS2HB
FullCovMat	50%	1.4	1.5	1.1	0.8
	90%	3.6	3.6	2.3	2.2
Kronecker	50%	1.4	1.5	1.0	0.8
	90%	3.7	3.8	2.3	2.2
NoRxCorr	50%	1.8	1.8	1.1	0.7
	90%	4.9	4.3	2.6	1.6
NoRXLxCorr	50%	1.8	1.8	1.1	0.8
	90%	4.8	4.4	2.5	2.2
NoTxRxCorr	50%	2.0	2.5	1.1	1.5
	90%	5.4	6.2	2.8	4.0
NoCorr	50%	1.9	2.4	1.1	1.4
	90%	5.4	5.7	2.9	3.9
FixTx0.25	50%	1.9	2.3	1.1	1.4
	90%	5.4	5.6	2.9	3.9
FixTx0.8	50%	1.7	2.1	1.0	1.2
	90%	4.7	5.1	2.5	3.3

smaller than that for the LB. For the LB the 50% deviation percentile is less than 2.5% in all cases, and less than 1.5% for the HB. The similar numbers for the 90% percentiles are 6.2% and 4.0%, respectively.

6. Conclusions

The overall objective has been to investigate to what degree details of the channel properties are necessary to predict the outage capacity (OC) for realistic designs and use of handsets, and possibly simplify their evaluation.

Based on numerous measurements involving two BSs, two frequency bands, and different persons and handsets in various use cases (UCs), it is found that a model assuming knowledge of the full covariance matrix results in 90% of the predicted median OC values at 15 dB SNR to be within about 6% of the correct value, with the Kronecker model achieving essentially the same accuracy. The accuracy depends on the outage capacity level (OCL) but is fairly insensitive around the median and lower than about 12% for levels in the 10–90% range for a 15 dB SNR.

It is emphasized that all the results take into account the joint impacts of the actual channel properties such as correlations and power distributions along the route for the individual handsets, usage, person, *etc.* The measured data were obtained in scenarios with both relatively high and low Tx-correlation coefficient (TxCC) (at the BS), which as expected turns out to be important for the modeling. Assuming a model with a fixed, incorrect TxCC leads to significantly higher relative error.

At the Rx end of the link (the user end) ten handsets were involved with different types of

realistic antennas and designs. In practice they generally have low branch correlation. Hence, assuming zero RxCC in a model instead of the correct values does not increase the error statistics for the OC significantly. Similarly, cross-link correlation coefficient (LxCC) values are typically small and assuming zero values in models does not change error statistics significantly.

These major findings of the paper are convenient from the point of view of MIMO handset performance evaluation. A relatively accurate estimate of the OC can be achieved from knowledge alone of the average power gain of each Rx-antenna/channel combination. Assuming a model with zero values for RxCC and LxCC, but correctly estimated TxCC, which may be noted to be independent of the handset, the median relative error of the estimated median OC is within 2.6% for 9 of the 10 handsets. Although one handset has a median relative error of 6.7%, due to an exceptionally high RxCC of about 0.7 in median, the errors may be considered small. These values are for a 15 dB SNR. For other SNRs of 5 dB, 10 dB and 20 dB the error may be slightly higher, with a maximum median error of up to 7.3%.

7. References

- [1] D. Astély, E. Dahlman, A. Furuskär, Y. Jading, M. Lindström, and S. Parkvall, "LTE: the evolution of mobile broadband," *IEEE Commun. Mag.*, vol. 47, no. 4, pp. 44–51, Apr. 2009.
- [2] D. Gesbert, M. Shafi, D. shan Shiu, P. J. Smith, and A. Naguib, "From theory to practice: An overview of MIMO space-time coded wireless systems," *IEEE J. Sel. Areas Commun.*, vol. 21, no. 3, pp. 281–302, Apr. 2003.
- [3] M. Murase, Y. Tanaka, and H. Arai, "Propagation and antenna measurements using antenna switching and random field measurements," *IEEE Trans. Veh. Technol.*, vol. 43, no. 3, pp. 537–541, Aug. 1994.
- [4] G. F. Pedersen, J. Ø. Nielsen, K. Olesen, and I. Z. Kovacs, "Measured variation in performance of handheld antennas for a large number of test persons," in *48th Vehicular Technology Conf., VTC '98*. IEEE, May 1998, pp. 505–509.
- [5] W. Kotterman, G. Pedersen, and K. Olesen, "Capacity of the mobile MIMO channel for a small wireless handset and user influence," in *Personal, Indoor and Mobile Radio Communications, 2002. The 13th IEEE Int. Symp. on*, vol. 4, Sep. 2002, pp. 1937–1941.
- [6] F. Harrysson, A. Derneryd, and F. Tufvesson, "Evaluation of user hand and body impact on multiple antenna handset performance," in *Antennas and Propagation Society Int. Symp. (APSURSI), 2010 IEEE*, Jul. 2010, pp. 1–4.
- [7] T. Zervos, K. Peppas, F. Lazarakis, A. Alexandridis, K. Dangakis, and C. Soras, "Channel capacity evaluation for a multiple-input-multiple-output terminal in the presence of user's hand," *IET Microw., Antennas Propag.*, vol. 1, no. 6, pp. 1137–1144, Dec. 2007.
- [8] F. Harrysson, J. Medbo, A. Molisch, A. Johansson, and F. Tufvesson, "Efficient experimental evaluation of a MIMO handset with user influence," *IEEE Trans. Wireless Commun.*, vol. 9, no. 2, pp. 853–863, Feb. 2010.
- [9] B. Yanakiev, J. Ødum Nielsen, M. Christensen, and G. Pedersen, "On small terminal antenna correlation and impact on MIMO channel capacity," *IEEE Trans. Antennas Propag.*, vol. 60, no. 2, pp. 689–699, Feb. 2012.

- [10] J. Ø. Nielsen, B. Yanakiev, I. Bonev, M. Christensen, and G. Pedersen, “User influence on MIMO channel capacity for handsets in data mode operation,” *IEEE Trans. Antennas Propag.*, vol. 60, no. 2, pp. 633–643, Feb. 2012.
- [11] V. Plicanic, H. Asplund, and B. K. Lau, “Performance of handheld MIMO terminals in noise- and interference-limited urban macrocellular scenarios,” *IEEE Trans. Antennas Propag.*, vol. 60, no. 8, pp. 3901–3912, 2012.
- [12] H. J. Song, A. Bekaryan, J. H. Schaffner, T. Talty, D. Carper, E. Yasan, and A. Duzdar, “Evaluation of vehicle-level mimo antennas: Capacity, total embedded efficiency, and envelope correlation,” in *Antennas and Propagation in Wireless Communications (APWC), 2014 IEEE-APS Topical Conference on*, Aug 2014, pp. 89–92.
- [13] T. Lankes, P. Turban, and F. Mierke, “Evaluation and optimization of LTE MIMO antenna configurations in automotive environment,” in *The 8th European Conference on Antennas and Propagation (EuCAP 2014)*, April 2014, pp. 1100–1104.
- [14] D. Gesbert, H. Bolcskei, D. Gore, and A. Paulraj, “Outdoor MIMO wireless channels: models and performance prediction,” *IEEE Trans. Commun.*, vol. 50, no. 12, pp. 1926–1934, Dec. 2002.
- [15] V. I. Piterbarg and K. T. Wong, “Spatial-correlation-coefficient at the basestation, in closed-form explicit analytic expression, due to heterogeneously poisson distributed scatterers,” *IEEE Antennas Wireless Propag. Lett.*, vol. 4, pp. 385–388, 2005.
- [16] K. T. Wong and Y. I. Wu, “Spatial-polarizational correlation-coefficient function between receiving-antennas in radiowave communications — geometrically modeled, analytically derived, simple, closed-form, explicit formulas,” *IEEE Trans. Commun.*, vol. 57, no. 12, pp. 3566–3570, December 2009.
- [17] V. I. Piterbarg, K. T. Wong, and Y. I. Wu, “Spatial correlation-coefficient across a receiving sensor-array — accounting for propagation loss,” *Electron. Lett.*, vol. 46, no. 19, pp. 1351–1353, Sept 2010.
- [18] C. S. Wang, M. Guo, K. T. Wong, and V. I. Piterbarg, “Fourth-order spatial correlation-coefficient across the uplink receiver’s spatial aperture — analytically derived in closed form,” *IEEE Trans. Commun.*, vol. 60, no. 3, pp. 724–734, March 2012.
- [19] M. Narandzic, C. Schneider, R. Thoma, T. Jamsa, P. Kyosti, and X. Zhao, “Comparison of SCM, SCME, and WINNER channel models,” in *Vehicular Technology Conference, 2007. VTC2007-Spring. IEEE 65th*, 2007, pp. 413–417.
- [20] P. Heino, J. Meinilä, P. Kysti, L. Hentilä, T. Jämsä, E. Suikkanen, E. Kunnari, and M. Narandžić, “D5.3: WINNER+ final channel models,” Wireless World Initiative New Radio WINNER+, Tech. Rep., 2010, available at <http://projects.celtic-initiative.org/winner+/>.
- [21] M. D. Estarki, J. X. Yun, Y. L. C. de Jong, and R. G. Vaughan, “Multiport antenna performance analysis from ray-traced channels for small cells,” in *The 8th European Conference on Antennas and Propagation (EuCAP 2014)*, April 2014, pp. 3305–3309.
- [22] Y. Jing, H. Kong, and M. Rumney, “MIMO OTA test for a mobile station performance evaluation,” *IEEE Instrumentation Measurement Magazine*, vol. 19, no. 3, pp. 43–50, June 2016.

- [23] P. Kyösti, T. Jämsä, and J.-P. Nuutinen, “Channel modelling for multiprobe over-the-air MIMO testing,” *Intl. Journal of Antennas and Propag.*, 2012.
- [24] J. Sanchez-Heredia, D. Pugachov, T. Bolin, and A. Gonzalez, “Antenna effect on LTE terminals exposed to realistic fading conditions,” in *Antennas and Propagation (EuCAP), 2013 7th European Conference on*, April 2013, pp. 1659–1663.
- [25] I. Vasilev, V. Plicanic, and B. K. Lau, “Impact of antenna design on MIMO performance for compact terminals with adaptive impedance matching,” *IEEE Trans. Antennas Propag.*, vol. 64, no. 4, pp. 1454–1465, April 2016.
- [26] W. Fan, J. Nielsen, O. Franek, X. Carreño, J. Ashta, M. Knudsen, and G. Pedersen, “Antenna pattern impact on MIMO OTA testing,” *Antennas and Propagation, IEEE Transactions on*, vol. 61, no. 11, pp. 5714–5723, Nov 2013.
- [27] P. Suvikunnas, J. Villanen, K. Sulonen, C. Icheln, J. Ollikainen, and P. Vainikainen, “Evaluation of the performance of multiantenna terminals using a new approach,” *IEEE Trans. Instrum. Meas.*, vol. 55, no. 5, pp. 1804–1813, 2006.
- [28] G. F. Pedersen, K. Olesen, and S. L. Larsen, “Bodyloss for handheld phones,” in *49th Vehicular Technology Conf., VTC’99*. IEEE, May 1999.
- [29] K. Boyle, “Mobile phone antenna performance in the presence of people and phantoms,” in *Technical Seminar: Antenna Measurement and SAR*. IEE Antennas and Propagation Professional Network, May 2002, pp. 8/1–8/4.
- [30] P. Vainikainen, M. Mustonen, M. Kyro, T. Laitinen, C. Icheln, J. Villanen, and P. Suvikunnas, “Recent development of mimo antennas and their evaluation for small mobile terminals,” in *Microwaves, Radar and Wireless Communications, 2008. MIKON 2008. 17th International Conference on*, May 2008, pp. 1–10.
- [31] J. Nielsen, B. Yanakiev, S. Caporal Del Barrio, and G. Pedersen, “On antenna design objectives and the channel capacity of MIMO handsets,” *IEEE Trans. Antennas Propag.*, vol. 62, no. 6, pp. 3232–3241, June 2014.
- [32] J. Ø. Nielsen, B. Yanakiev, S. C. D. Barrio, and G. F. Pedersen, “Channel statistics for MIMO handsets in data mode,” in *The 8th European Conference on Antennas and Propagation (EuCAP 2014), April 2014.*, 2014, pp. 2818–2822.
- [33] B. Yanakiev, J. Nielsen, M. Christensen, and G. Pedersen, “Long-range channel measurements on small terminal antennas using optics,” *IEEE Trans. Instrum. Meas.*, vol. 61, no. 10, pp. 2749–2758, Oct. 2012.
- [34] J. Ø. Nielsen, J. B. Andersen, P. C. F. Eggers, G. F. Pedersen, K. Olesen, E. H. Sørensen, and H. Suda, “Measurements of indoor 16×32 wideband MIMO channels at 5.8 GHz,” in *Proceedings of the 2004 Int. Symp. on Spread Spectrum Techniques and Applications (ISSSTA 2004)*, 2004, pp. 864–868.
- [35] C. Oestges, “Validity of the Kronecker model for MIMO correlated channels,” in *Vehicular Technology Conf., 2006. VTC 2006-Spring. IEEE 63rd*, vol. 6, May 2006, pp. 2818–2822.
- [36] H. Shin, M. Win, J. H. Lee, and M. Chiani, “On the capacity of doubly correlated MIMO channels,” *IEEE Trans. Wireless Commun.*, vol. 5, no. 8, pp. 2253–2265, Aug. 2006.